Polymer Morphology of CO_2-Blown Rigid Polyurethane Foams: Its Fractal Nature

H. J. M. GRÜNBAUER[1,*] and J. C. W. FOLMER[2]

[1]Urethane Polymers R&D, [2]Analytical Development Department, Dow Benelux NV, P.O. Box 48, 4530 AA Terneuzen, The Netherlands

SYNOPSIS

Small-angle x-ray scattering (SAXS) and transmission electron microscopy (TEM) have been applied to study polymer morphologies of CO_2-blown rigid polyurethane foam samples of varying isocyanate index. The results are consistent with an irregular (meso)phase segregated structure with phase boundaries showing fractal symmetry. Phase segregation persists throughout the index range, although the interfacial surface tends to smoothen with increasing isocyanate index to eventually result in a significant degree of energetic 'sharing' across the phase boundary. The latter can satisfactorily be explained by a free volume double layer (FVDL) model. Mechanistically, fractal symmetry was attributed to the competition between crosslinking and phase segregation tendencies in rigid PU foam polymers. The resulting frozen-in morphology represents an early stage of the development towards a more regular spinodal phase segregation, as occurring in polyurethane foam systems of lower crosslink density (e.g. flexible foams). © 1994 John Wiley & Sons, Inc.

INTRODUCTION

Rigid polyurethane (PU) foams find wide application as high-quality thermal insulation materials, for example, in refrigerators, freezers, and laminated panels for building insulation. Typically, the foams are produced by catalyzed reaction of multifunctional polyalkeneoxide oligomers or 'polyols' with oligomeric methyldiphenyl iscocyanate or 'polymeric MDI.' The result is a highly crosslinked polymer network. The heat generated during polymerization is largely sufficient to vaporize a low boiling physical blowing agent that is added to the polyol formulation. Together with appropriate foam stabilizing surfactants, this blowing agent is responsible for the formation of an expanded fine close-celled material during polymerization.

Traditionally, trichlorofluoromethane or CFC-11 has been the blowing agent of choice, due to its excellent thermal insulation properties, low toxicity, and favorable boiling point of 24°C. However, present concerns over the destruction of the earth's ozone layer have imposed an urgent need for alternative technologies yielding foams of similar, outstanding thermal resistance performance.

One of the most attractive alternative routes comprises generation of CO_2 via the isocyanate-water reaction. This reaction produces an unstable carbamic acid that decomposes to give CO_2:

$$R-N=C=O + H_2O \rightarrow (R-NH-CO_2H) \rightarrow R-NH_2 + CO_2 \nearrow \quad (1)$$

The resulting aromatic amine quickly reacts with isocyanate to give an urea linkage:

$$R-NH_2 + R-N=C=O \rightarrow R-NH-CO-NH-R \quad (2)$$

Reduction or even total replacement of CFC-11 blowing would, thus, be simply attainable by increasing the water level of the polyol formulation.

The main obstacle preventing straight-forward implementation of this technology is the relatively

* To whom correspondence should be addressed.

Journal of Applied Polymer Science, Vol. 54, 935–949 (1994)
 CCC 0021-8995/94/070935-15

fast outward diffusion of CO_2, which is measurable as a rapid loss of thermal insulation value with time.[1]

A recent article by Kaplan et al.[2] emphasized the impact of polymer chemistry on CO_2 and O_2 diffusion processes. Its objective was to derive structure/permeability correlations for future development of improved urethane polymers. Morphological aspects were not considered, as the article focused on the chemical structure of the resins. Recent diffusion studies[3-5] indicated, however, that diffusivity in urethane elastomer membranes also strongly depends on parameters characterizing their morphology. This is particularly true at scales just above monomeric sizes (the nano or meso range). In the highly crosslinked urethane/urea copolymers resulting from reactions (1) and (2) above, morphology in this resolution range is likely to be of similar importance. (To avoid confusion with any morphological features in the micron range, we refer to mesophase rather than microphase morphology.)

It seemed worthwhile, therefore, to study the mesophase morphology of rigid PU foam polymers. In contrast to flexible PU foam polymers,[6-8] the polymer backbone of rigid PU foams has hitherto not been elucidated in any detail. Small-angle x-ray scattering (SAXS) was selected as the technique of choice because, for flexible foams, this technique has often yielded important morphological information on the nanometer scale. At the onset of our study it was by no means clear how to extend the application of SAXS to rigid formulations. Previous studies on comparable systems[8] as well as our own preliminary data have revealed[10] that rigid SAXS patterns lacked the scattering maximum typical for domain structures. At the time, such patterns defied interpretation following classical theories, beyond the general statement that the usual (domain) phase segregation was absent or incomplete.

In recent years, considerable knowledge has emerged on the relationship between fractals, scattering, and phase separation, particularly in systems far from equilibrium.[11] This prompted the attempt of a fractal approach to the current study, which appears to have been succesful, though an extension of the theory to include the presence of a free-volume double-layer, had to be developed to account for the total range of scattering data.

EXPERIMENTAL

Foam Samples

All foam samples were cut from the core of $20 \times 20 \times 20$ cm^3 cubes of foam prepared in cardboard boxes. The foams were prepared by a handmix technique using 4 s stirring at 3000 rpm to mix polyol and isocyanate ingredients. Free-rise density was consistently kept at 20 kg/m^3. Plaques prepared in the absence of H_2O were used as prepared.

Foams were prepared at step-wise increasing isocyanate index, defined as:

$$\text{Index} = \frac{[\text{NCO}]}{[\text{Act(H)}]} \tag{3}$$

where [NCO] and [Act(H)] represent, respectively, the concentration in molar equivalents/liter of isocyanate groups and 'active' hydrogen-bearing groups capable of reaction with isocyanates, such as —OH and NH_2 groups. In this way, the problem of on-line kinetic measurements during the short foam-rising period of approximately 1 min could be avoided. In SAXS experiments, this approach is indispensible, as it would be virtually impossible to record relevant kinetic events within 1 min by means of the usual type of laboratory x-ray sources.

Except when otherwise stated, a blend comprising two different polyols was used to produce the foams studied: a high molecular weight polyol serving to lower the viscosity of the polyol blend and a high-functional polyol for crosslinking. Throughout this work, the former is indicated as 'viscosity reducing' or 'low viscosity' polyol, while the remainder of the polyol blend is indicated as 'high-functional base' polyol. Voranate* M220, a polymeric MDI type, was always used at the isocyanate side, except for a series of model foams where Voranate* M125 (4,4'-methyldiphenylisocyanate) was employed.

Small-Angle X-Ray Analysis

SAXS profiles were obtained by photography (Kodak direct exposure x-ray film). An Anton Paar pinhole camera was used with 250 mm camera length, mounted on an ordinary generator equipped with a copper tube, operated at 50 kV and 30 mA. During exposure, the camera was evacuated. Exposure times varied from 1.6 to 16 h. The photographs were digitized (typically 200 by 200 data points) using a LKB Ultroscan XL raster densitometer. After establishing the center of symmetry of the pattern by a nonlinear regression routine, averaging was performed over data, the radii of which fall in a segment. A robust routine, using medians and median absolute deviations, was used first. It removed any outlying,

* Trademark of the Dow Chemical Company.

nonisotropic data such as the shadow of the beamstop. It also largely suppressed the residual parasitic pattern. As the collimator contains a third intercepting pinhole, the latter is limited to a few streaks in a narrow zone just outside the beamstop.

The linearity of the densitometer was ascertained by means of a Kodak grey scale. The linearity of the films was ascertained by stacking two pieces of film in the cassette and coexposing them. A plot was made of the top pattern vs. the second for equal q values. A straight line was observed until the top film reaches O.D. values approaching 3.00. Soon after that, total saturation is observed. The slope of the plot is about 3, due to the attenuation of the second pattern by the first film. In the data processing, all data above O.D. = 3 were discarded and a very minor saturation corrrection performed on the rest. ($D_{sat} = 12$).

A simple constant was subtracted from the data to correct for the combined effects of fogging and background scatter. To this purpose, an area of 20 by 20 data points was selected in the tail of our photograph to derive a background value. Contrary to classical Porod analysis, most of our log–log analysis is performed at relatively small values of q, where the pattern is strong compared to the linear contribution to the background. Nonlinear contributions are smaller yet and negligible in this range. All intensities are represented on a relative scale. They are either shown in log–log fashion or represented after correction for a Lorentz (q^2) term, where q denotes the scattering vector $q = 4\pi \sin \Theta/\text{lambda}$ expressed in nm^{-1}. Part of our discussion concerns the disappearance c.q. absence of any signal that could possibly be construed as a classical domain peak. Our use of the Lorentz correction simply represents a 'worst case' scenario, because peaks are more easily seen than prior correction.

Microscopy

Samples for TEM analysis were prepared by embedding 3 × 3 × 15 mm sized foam samples in low viscosity epoxy resin, followed by overnight curing. A Leica ULTRACUT E ultramicrotome fitted with a diamond knife was used to cut 50 nm sections from a trapezium-shaped embedded mesa. Unstained thin sections were collected on a copper grid and examined in a Philips EM400T at 120 kV. No further staining, coloring, or etching was applied. Observed features are, therefore, entirely due to differences in electron density.

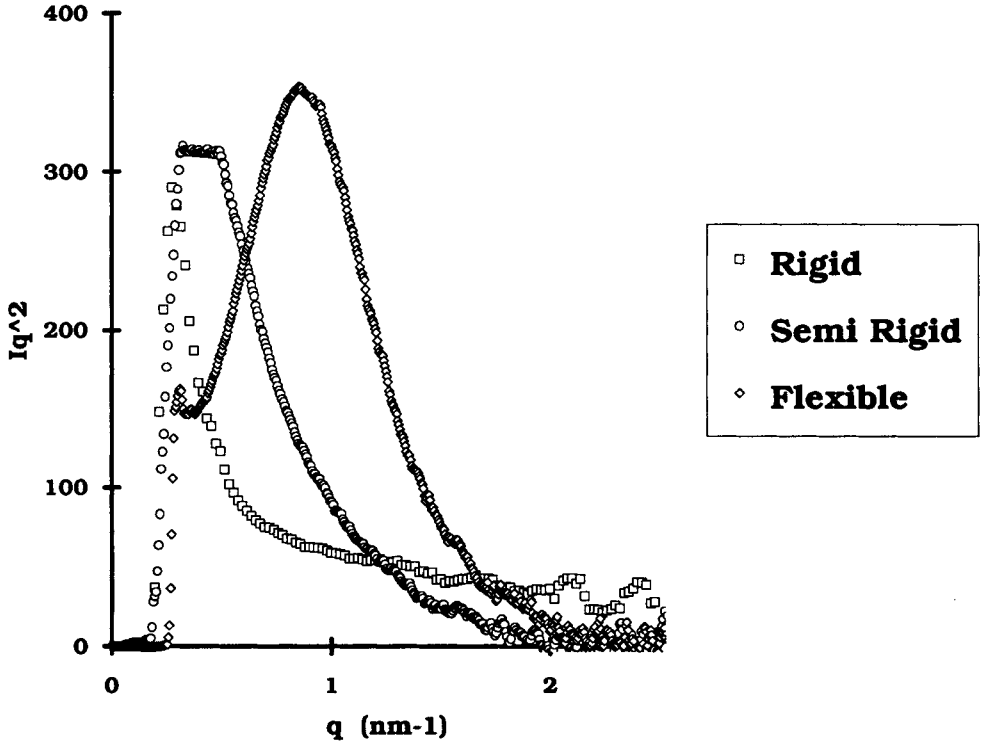

Figure 1 Typical SAXS profiles of rigid, semirigid, and flexible polyurethane foams.

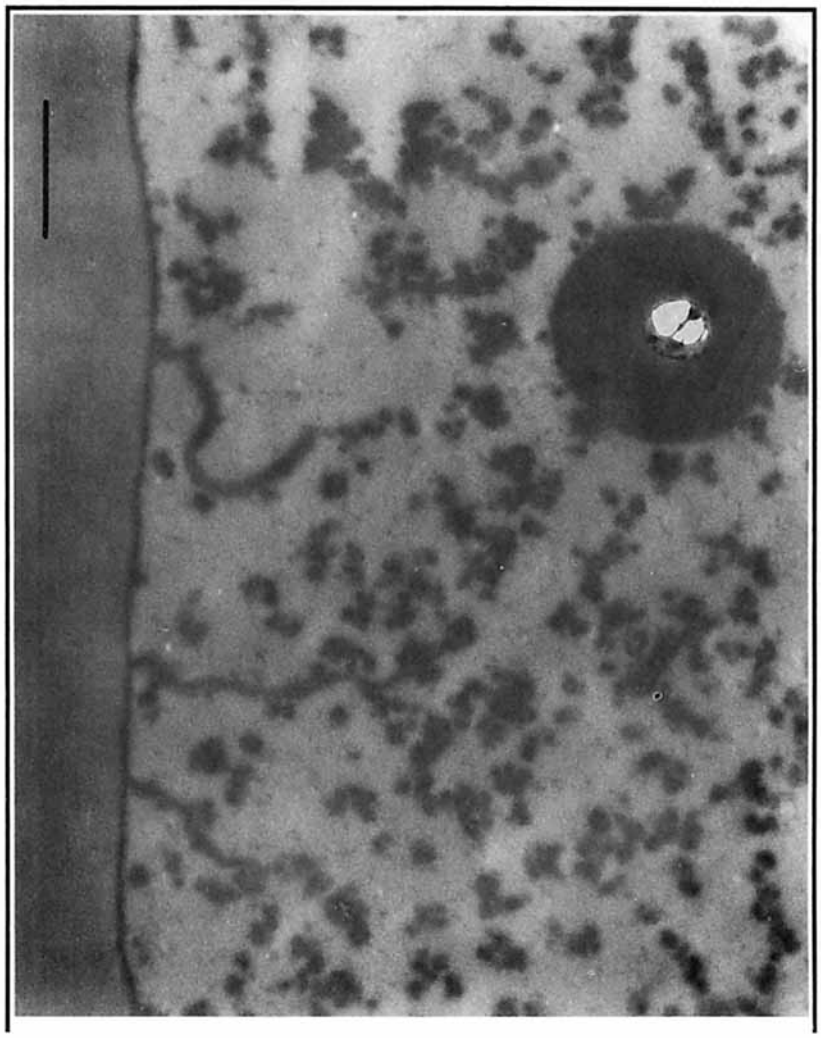

Figure 2 TEM micrographs of water-blown foams at step-wise increasing values of the isocyanate index: (a) I = 0.3, (b) I = 0.4, (c) I = 0.5, (d) I = 0.6, (e) I = 0.7, (f) I = 0.8. Magnification: 30000×, bar length = 1 micron.

RESULTS AND DISCUSSION

Flexible vs. Rigid Morphologies

Figure 1 summarizes scattering profiles measured for typical rigid, semirigid, and flexible foams, all represented on a relative scale after correction for a Lorentz (q^2) term. In agreement with literature data,[6-8,12] the flexible all water-blown foam shows a clear intensity maximum at $q = 0.85$ nm^{-1}, corresponding to a domain period of 7.5 nm. In contrast, intensity maxima are absent in the rigid foam pattern. The scattering pattern of the semirigid foam reveals an intermediate type of behavior with a shoulder around $q = 0.5$ nm^{-1}, indicating a tendency towards formation of regular domain structures that can be detected by SAXS. This is undoubtedly due to its polyol composition: a blend of a 6000 molecular weight viscosity reducing polyol with the base polyol from the rigid foam formulation.

This overall type of sequence in the scattering pattern is well known from literature on urethane elastomers. Van Bogart et al.,[13] for example, reported very similar effects for polycaprolactone/polyurethane copolymers with varying soft segment molecular weight.

One could argue in principle, that a scattering maximum in the rigid foam profile is hidden below the instrumental cut-off point at 0.30 nm^{-1}. This would require the presence of a much larger domain periodicity than in flexible foams, similar to those hypothesised by T. P. Russell et al.[14] for some of

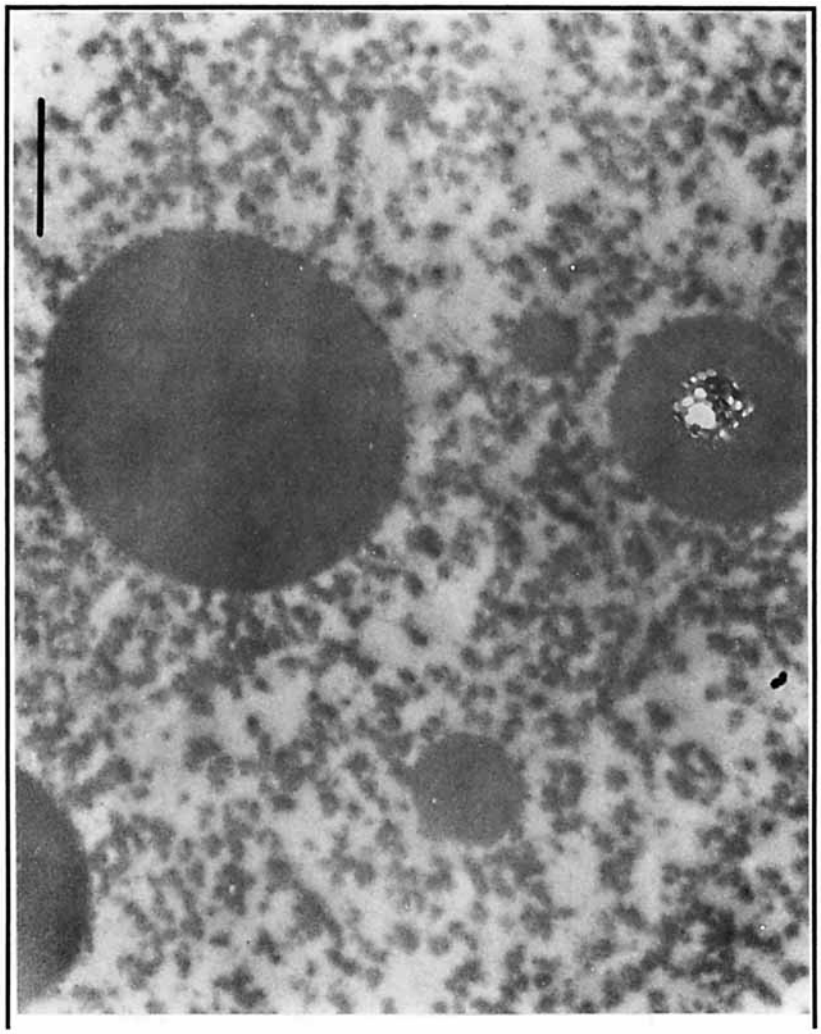

Figure 2 (*Continued from the previous page*)

their interpenetrating networks. To investigate the morphology in more detail at lower resolutions than those accessible in SAXS, foam samples have been submitted to TEM analysis.

TEM on Rigid Morphologies

TEM results [Fig. 2(a–f)] typically show irregularly spaced dark spots of about 50–300 nm, the number of which increases with increasing isocyanate index until, at index 0.7, individual spots can no longer be distinguished. They merge into a continuous phase, though a boundary between a light and a dark phase can still be discerned. At even higher values the image becomes almost—but not quite—homogeneously dark, like black marble. Phase boundaries become hard to distinguish, but this could be an optical illusion, as at some point the dark phase may have become the continuous matrix phase (phase inversion). Projection (superposition) effects through the 50 nm thick sample could make it difficult to distinguish the lighter dispersed (embedded) phase in such a case.

A few much larger spots of about 1000–5000 nm are visible as well, especially in the 0.3 and 0.4 index samples. Their spherical shape as well as their size make these larger spots rather reminiscent of the dispersion of isocyanate droplets in polyol that emerges immediately after mixing a low index formulation. We, therefore, tentatively assign this morphological feature to a primary (i.e., as present from before the polymerization) as opposed to a secondary inhomogeneity (i.e., as resulting from/during the polymerization). Of course, that is not

Figure 2 (*Continued from the previous page*)

to say that the large 'droplets' have remained unaltered during the reaction in a chemical sense, just that the morphological shapes we observe, probably stem from before that event.

At low index the smaller 'spots' look like isolated islands superficially, but they could, in fact, form part of a more or less continuous web-like structure. This can be inferred from the fact that the smaller 'spots' converge to a dense network when the index is increased (i.e., when more urea and urethane can be formed). We tentatively assign this feature to a urea/urethane network precipitate, therefore. In this view ,this inhomogeneity is clearly of a secondary nature.

This interpretation is sustained by the observation that, in contrast to CFC-blown foams, water-blown foam shows very little tendency to collapse, even at very low index.[10] Results of extraction experiments furthermore allow to identify the precipitated fraction at low index as comprising polyurea from reaction (2) in conjunction with a growing polyurethane network.[10]

SAXS Patterns of Rigid Systems

From the analysis of the microscopy data, the onset at which SAXS would be able to detect scattering from the precipitate should be found in the scattering vector range of $0.02 \leq q \leq 0.1$ nm^{-1}, below the instrumental cutoff at 0.3 nm^{-1}. In the accessible q range of 0.3 to 2.5 nm^{-1}, the scattering (caused by 2 to 20 nm sized objects) should, therefore, correspond to the fine structure of the spots. We can only speculate what the most probable SAXS pattern in

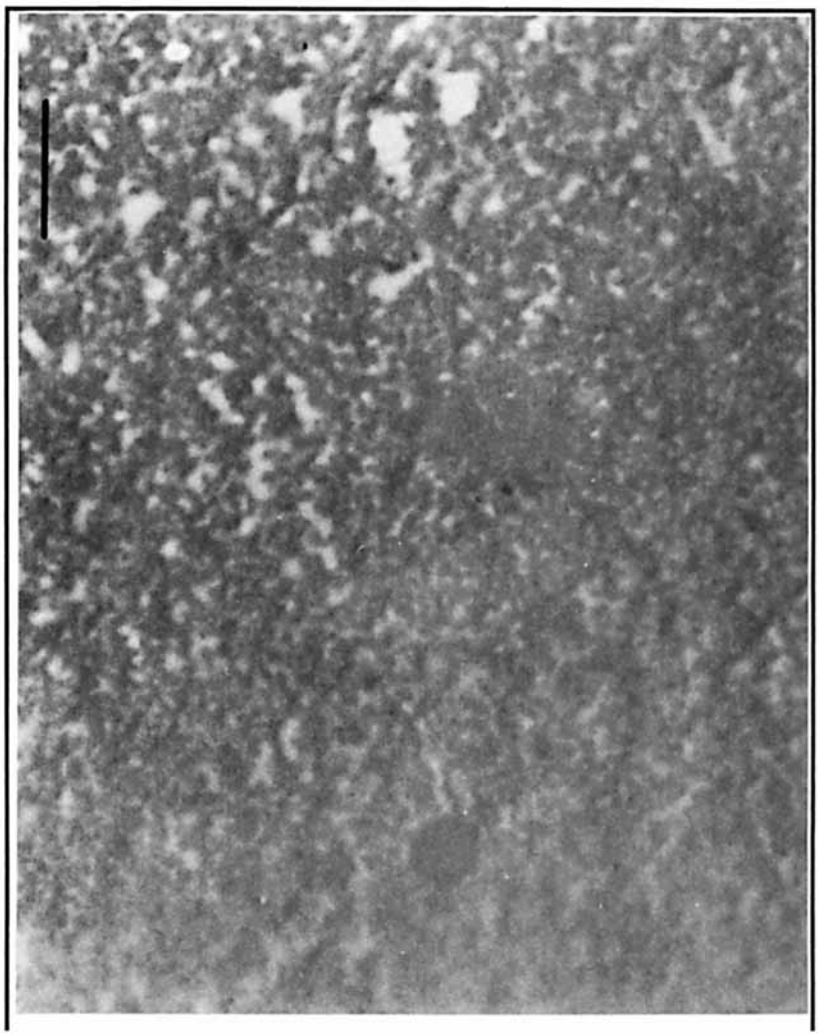

Figure 2 (*Continued from the previous page*)

the 0.02–0.1 nm^{-1} range is, but due to the random distribution of the spots, a bona fide maximum is rather unlikely. Saturation to a plateau value seems more likely.[15]

SAXS patterns as typically seen in the observable range, monotonically decreasing without a maximum, have occasionally been described in the urethane literature.[8,9,14,16] They are rather scarce, however, and to our knowledge, none have been published for rigid urethane foam systems. Undoubtedly, the scarcity is in part explained by the fact that rigid systems are such dauntingly complex resins from a chemical point of view, but there is a different reason as well.

The dominant interpretational framework of SAXS on condensed systems has long been a model involving an ordered domain type segregation with a well-defined long period. Our patterns clearly cannot be interpreted as resulting from such a system. For those few urethane foam systems for which monotonic patterns have been reported in the past, they are, indeed, interpreted as a negative result, in the sense of indicating the absence of segregation (phase mixing).[5,8,9] Unfortunately, it is hard to see how an interpretation in terms of phase mixing can be reconciled with the microscopy data for our systems, certainly for the lower part of the index range.

However, with the emergence of fractal scattering theory, different—less orderly—types of segregated morphologies are no longer beyond the scope of existing SAXS theory.[17] This means that phase segregation of a more disorderly nature (as opposed to phase mixing) represents a possible interpretation. In addition, it was shown[18] that fractal theory pro-

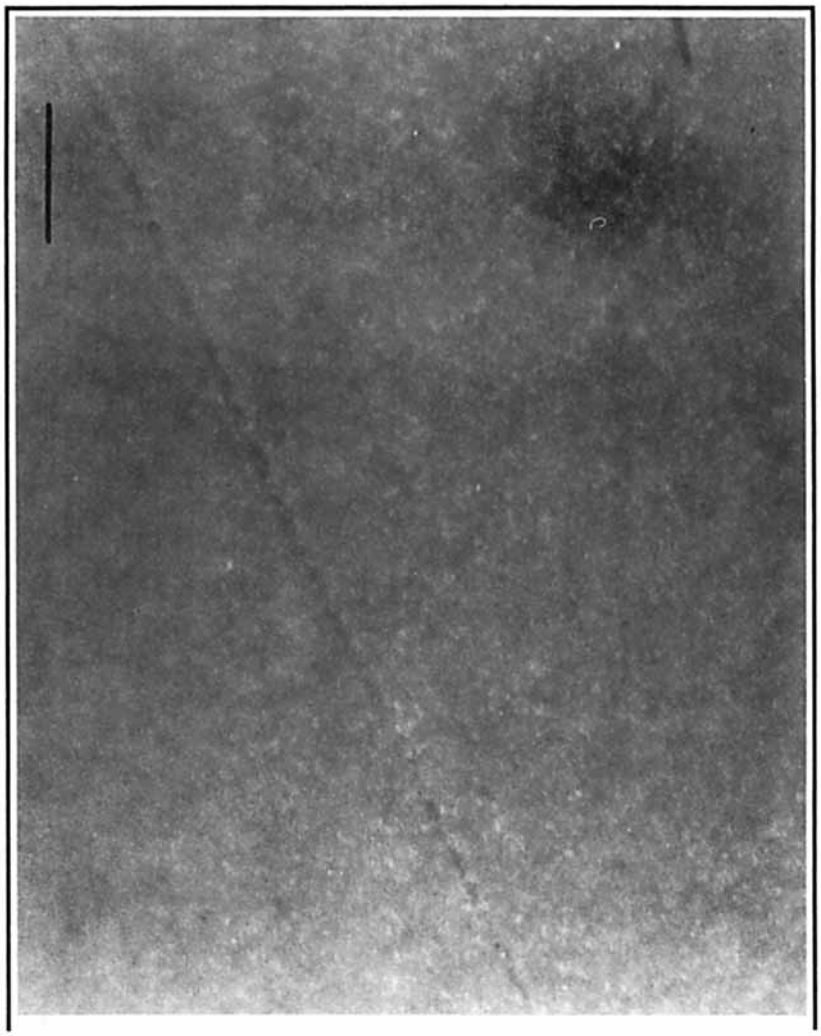

Figure 2 (*Continued from the previous page*)

vides a much desired framework for the understanding of the structure of highly crosslinked polymer networks. Our systems are a complex example of this general class. The SAXS data were, therefore, examined with fractal segregation in mind.

Fractal Interpretation of Rigid Patterns

Figure 3 shows that our SAXS results are, indeed, perfectly amenable to fractal analysis. Adopting fractal practice[17] the patterns are now represented in a log–log fashion. In this representation, they show a straight-line behavior, apart from a few exceptions described below. Figure 3 gives an example showing a series of SAXS patterns, with a step-wise increment of the isocyanate index. As a rule, the slope becomes steeper with the isocyanate index, but the exact progression depends on the constituents of the formulation, both polyol and water. Most patterns required modest exposure times only, comparable to those used for typical flexible foams. For the lowest value of the index, however, the patterns tend to be rather weak.

According to fractal scattering theory,[17] the linearity over 1 to 2 decades of the $\ln(I)$ vs. $\ln(q)$ plots is explained in terms of a morphology exhibiting fractal symmetry. The slopes of the curves are directly related to its fractal dimension.[17] Similar to a polymer in solution, a phase mixed system should give a flat curve or present slope values less negative than -3. These are taken to represent a mass fractal, essentially a single phase with internal inhomogeneities in varying state of clustering. Values between -3 and -4 represent a surface fractal, i.e., a

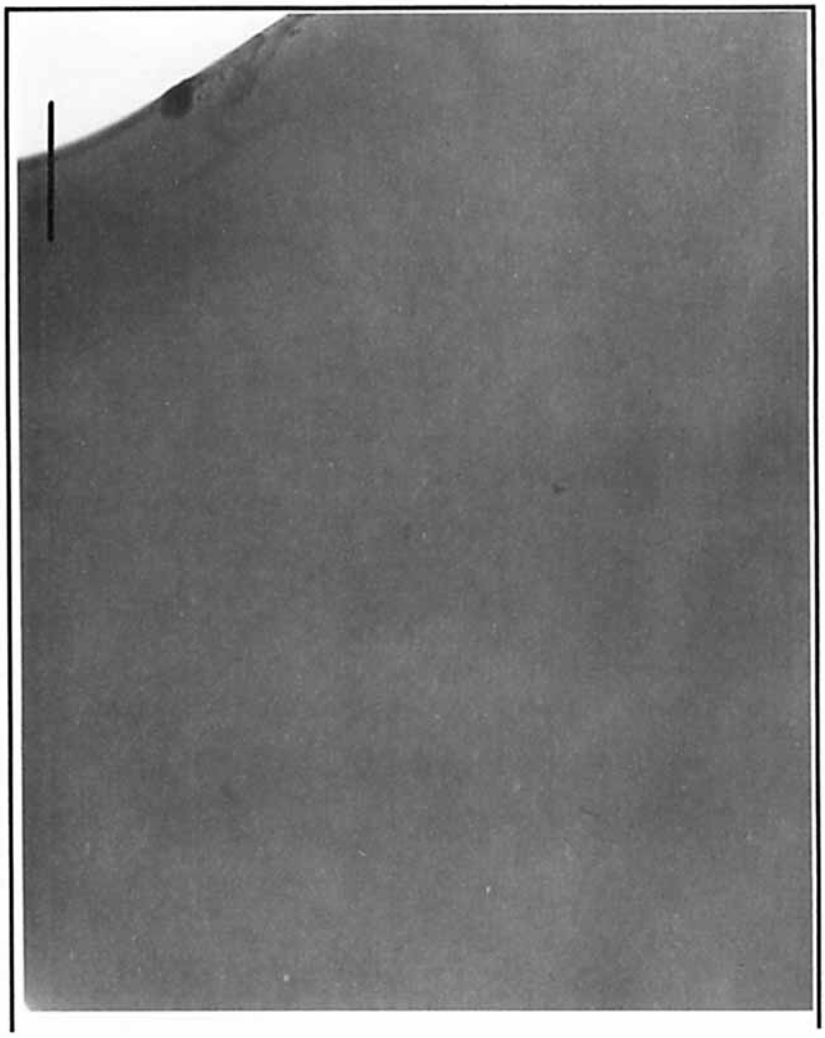

Figure 2 (*Continued from the previous page*)

two-phase system, the degree of segregation of which expresses itself in an interface of varying degree of roughness.

This interpretation implies that the patterns are by no means devoid of morphological information. Nor are the systems phase mixed: virtually all slopes are more negative than −3. Furthermore, useful qualitative information is obtained from the development of fractal dimensionality as a function of index. As a general trend, the slope values become more negative with the index. One could look upon this as a progression towards more and more complete phase segregation. If the assumption is made that sample morphology at consecutive indices reflects real-time morphology development during foam rise, this is useful information, indeed. Extending the approach, the morphological effects of the various constituents, both polyol and water, have been studied by monitoring SAXS pattern slope values of their individual reaction products with polymeric isocyanate.

The Role of Polyol Constituents without Water

Figure 4 represents fractal slope values as a function of index determined for polymer plaques in the absence of water. In all instances, the SAXS patterns showed fractal symmetry with a tendency towards steeper slope values as isocyanate index increases. Substantial overlap is observed between the curves for the total polyol blend and the viscosity cutting polyol alone. Both are descending from about −3 to (somewhat beyond) −4, which corresponds to a transition from a mass fractal or surface fractal of

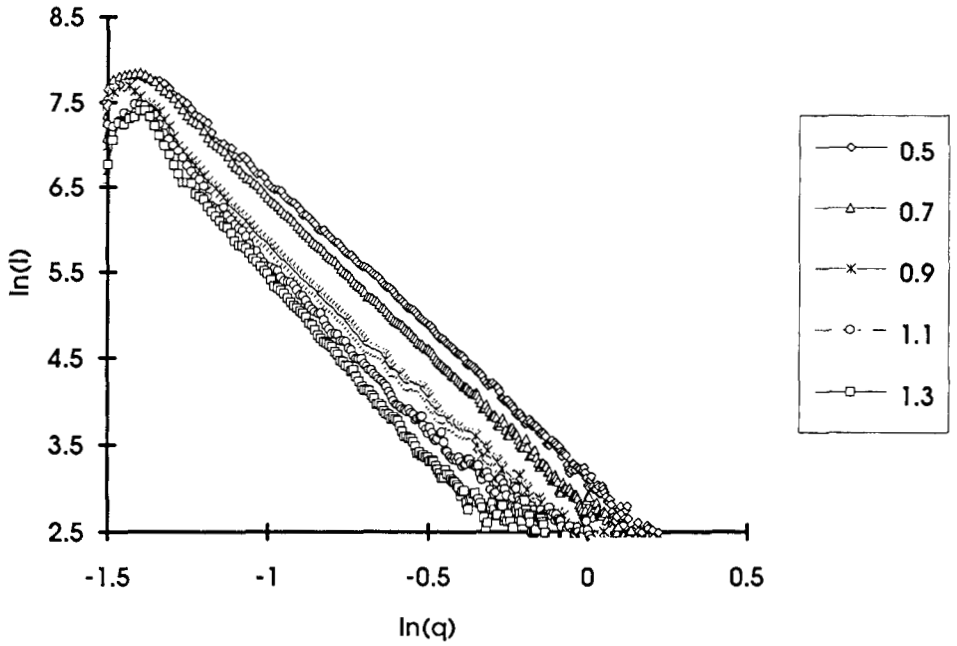

Figure 3 Typical monotonic SAXS profiles at various values of the isocyanate index, showing fractal self-similarity.

dimension 3 to a surface fractal of dimension 2. Morphologically, this implies that the surface roughness of the phase boundary is decreasing with increasing index to yield rather smooth surfaces at index 0.9. The persistance of fractal scattering at higher indices indicates that the phase boundaries do remain intact and that the apparent homogeneity in the TEM image is, indeed, an illusion.

Scattering curves for the base polyol without water present a special case, however. Very steep slopes are observed that are not interpretable using classical fractal theory alone. The slope values in Figure

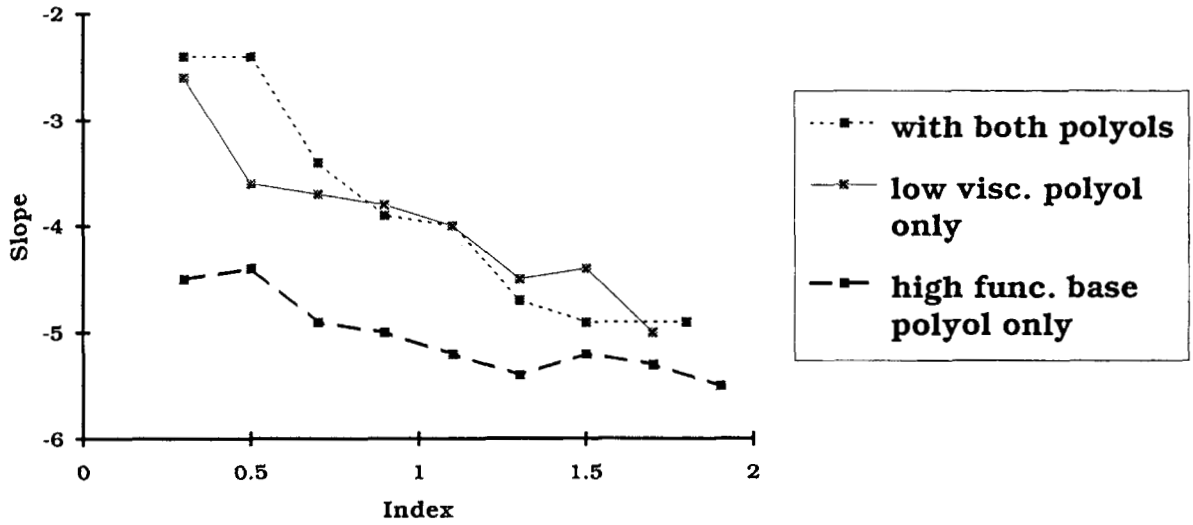

Figure 4 Fractal slope values as a function of isocyanate index for SAXS profiles of polymer plaques prepared in the absence of water.

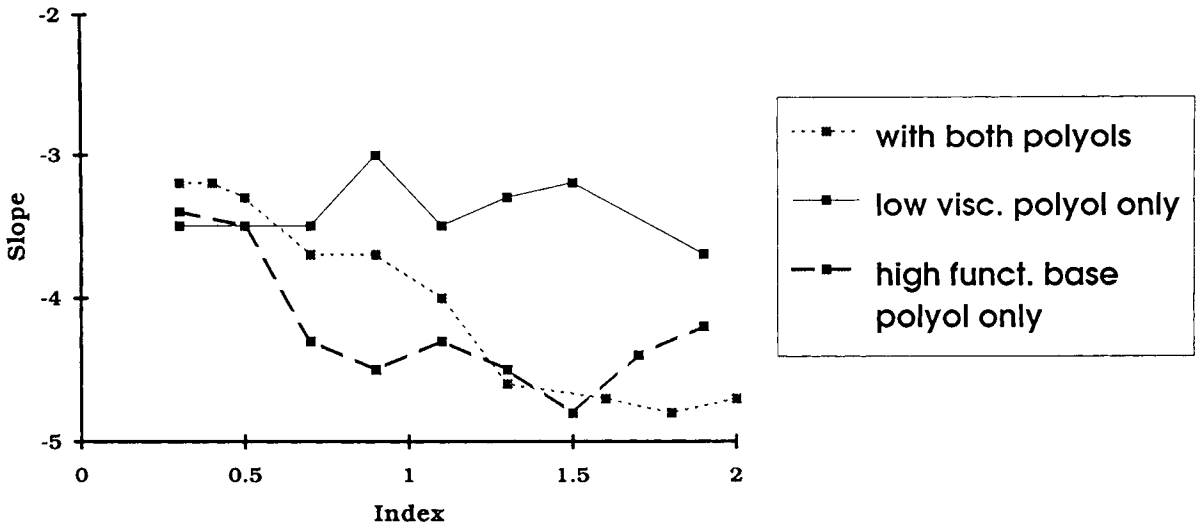

Figure 5 Fractal slope values as a function of isocyanate index for SAXS profiles of rigid foams.

4 range from −4 to −5.5, implying a transition from a surface fractal of dimension 2 to one of dimension −0.5, which is physically impossible. It was precisely for this type of data that a new theoretical approach was developed (cf., Appendix I and ref. 19) that allows us to model this type of extreme slope values in terms of free-volume double layers (FVDL) between segregated phases.

An alternative model that invokes diffuse (phase mixed) boundaries does exist (the Ruland model[20,21]). It does explain a steeper decay of the scattering curve, but no longer allows fractal linearity in a log–log plot. As the broad picture of all data is one of steepening slopes with the index, i.e., a tendency towards more profound segregation, it seems rather illogical to invoke a partial remixing at the end of this process for one series in particular. For this reason, we prefer the FVDL model that retains the fractal signature and assumes complete segregation, albeit with a measure of energetic 'sharing' (mutual strain) across the phase boundary (cf., Appendix I), a full account is given elsewhere.[19]

Incorporating the FVDL model into our interpretation, a consistent picture emerges. The high-functional base polyol patterns can be understood in terms of a competition between crosslinking and a strong phase segregation tendency. The result is a system with a disordered precipitate with a highly strained interface, visualized as a free-volume double layer. Addition of the low viscosity polyol reduces the weight average functionality of active groups. It will, thus, delay the NCO conversion at gel which, in turn, allows phase separation to occur over a greater NCO conversion domain. This results in a reduced buildup of interfacial strain. Scattering patterns in the presence of the low-viscosity polyol are, therefore, back to less extreme slope values.

Foams in the Presence of Water

Slope values for foams in the presence of water are shown in Figure 5 where, again, substantial overlap is found, now between the curves for the total blend and the base polyol. The deviating curve for the low viscosity polyol plus water is at least in part explained by the shape of the scattering pattern as represented by Figure 6. This pattern is the clearest example amongst our data where fractal linearity was broken by a 'kink.' Adjacent members of this series show minor signs of nonlinearity as well. Most likely this foam should be qualified as tending towards a flexible type due to the preeminence of low viscosity polyol. Its dilution effect is apparently strong enough to allow some incipient ordering of the precipitate's structure.

In the presence of base polyol, by contrast, the patterns are dominated by polyurea formation without losing their characteristic fractal behavior.

The Overall Picture

Fractal SAXS patterns have been reported in other highly crosslinked polymers.[18] The question why they occur in rigid urethane foams is probably best

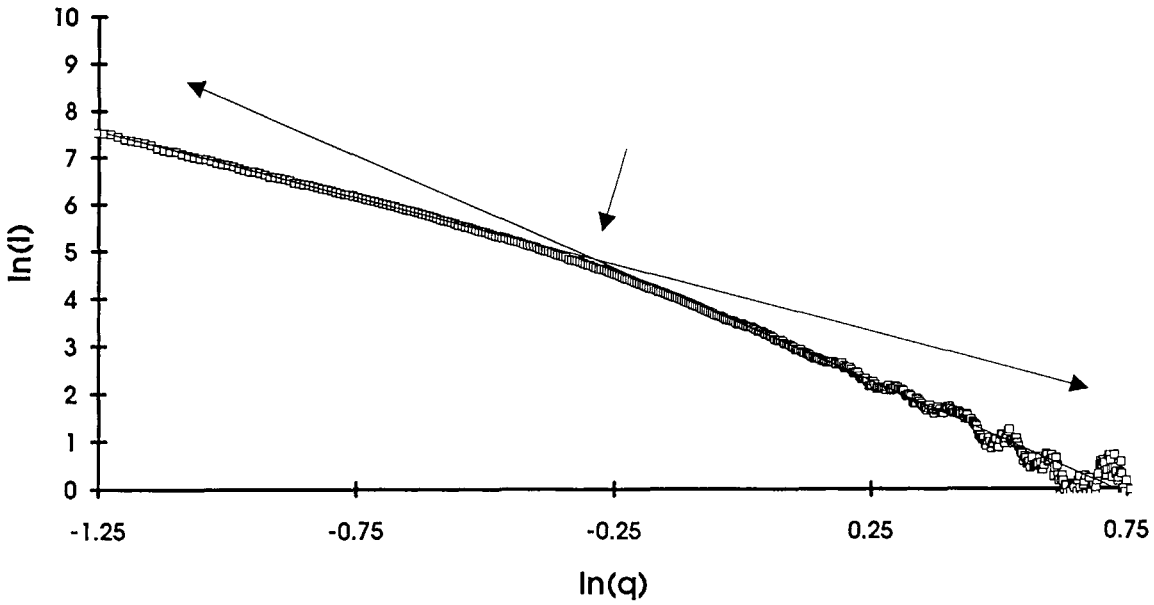

Figure 6 SAXS profile at I = 0.7 of a plaque from low-viscosity polyol in the absence of water showing the clearest example of a break in the linearity of the rigid foam SAXS patterns.

answered by considering their position in relation to the total spectrum of urethane polymers. Starting from thermoplastic urethanes, it will be clear that, in the absence of crosslinking, hard segments possess sufficient mobility to follow the thermodynamically determined tendency for phase segregation, most likely by a spinodal type mechanism.[12] It leads to the well-known domain structure with its consid-

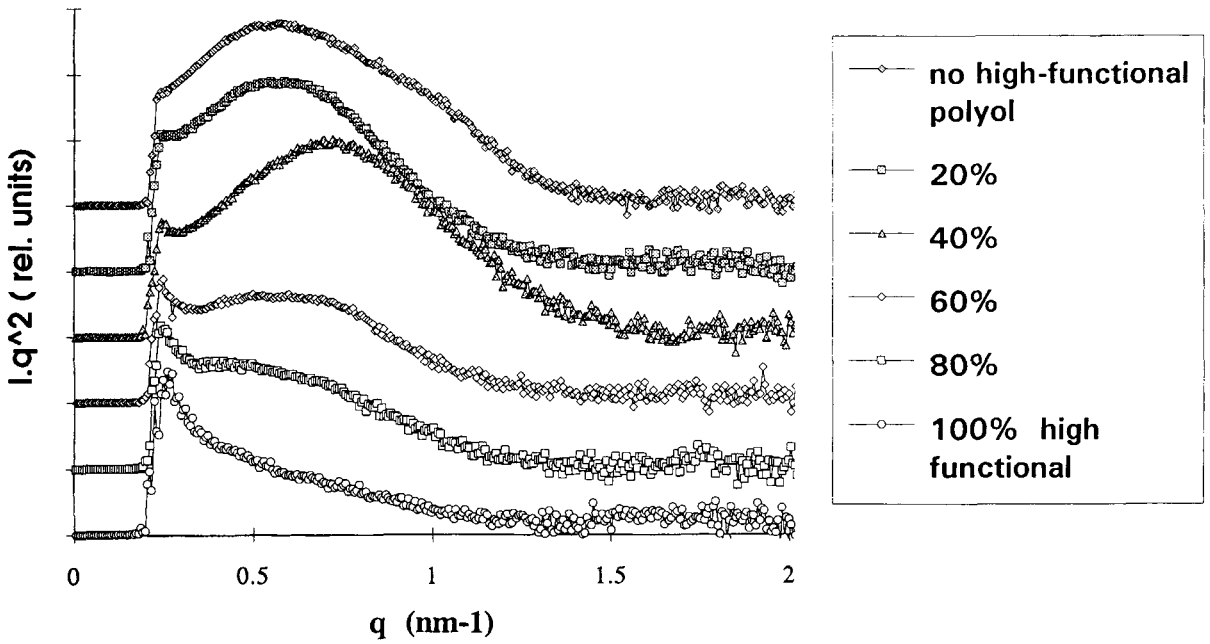

Figure 7 Lorentz-corrected SAXS patterns for rigid foams prepared from blends of a base polyol and its monol counterpart showing the transition from a monotonic pattern to a classical Long Period pattern.

erable degree of regularity. For flexible urethane foams, crosslinking is still insufficient to effectively hamper a regular phase segregation of this type. In rigid foams, due to the presence of high-functional base polyol and polymeric isocyanate, phase segregation is seriously frustrated by a strong crosslinking tendency. The low viscosity polyol mitigates these effects to some extent by releasing interfacial strain. On the whole, however, phase segregation, though it does occur, proceeds far from equilibrium in rigid foam polymers, leading to a much more irregular structure.

Figure 7 nicely illustrates these views. This figure represents Lorentz-corrected SAXS patterns of rigid foams prepared from 4,4′-MDI and a blend of a high-functional base polyol and its monofunctional polyether counterpart (i.e., a 'monol'), mixed in various proportions. At 100% monol, crosslinking is totally absent. The reacted species are, consequently, linear, and their mobility is sufficient to allow rearrangement into regular domains. At base polyol levels above 50%, the intensity maximum starts to collapse as regular domain formation is increasingly hampered by crosslinking of the multifunctional base polyol. At 100% base polyol, this tendency ultimately leads to the typical monotonic pattern observed for all rigid foam polymers studied sofar.

As pointed out in literature,[11] in systems far from equilibrium, undergoing a spinodal event, a ramified, fractal state of segregation is, indeed, expected to preceed the actual onset of the spinodal, more regular, segregated structure. If this view holds, one could regard the system as one where the eventual spinodal ordering is suppressed by the high crosslink density emerging during the reaction. The morphology is, consequently, frozen in its primeval fractal state of segregation. Extrapolating this view, it is to be expected that a fractal phase occurs at some point during the early stages of flexible PU foam formation as well.

The occurrence of a strained free-volume double layer is a new element in this context. It is reported here for the first time and presents a necessary element to arrive at a consistent overall picture. In fact, in contrast to the diffuse boundary model, it emphasizes how these systems insist on segregation against all constraints imposed by the crosslinking.

CONCLUSIONS

For the first time, SAXS patterns of rigid PU foam polymers have been analyzed in a consistent manner to yield a qualitative view on the development of their morphology. The fact that this proved feasible is probably the most important conclusion of our study as far as the methodology is concerned. Equally important is the emerging picture of the morphology itself: an irregular (meso)phase segregated structure with phase boundaries showing fractal self-similarity. Phase segregation persists throughout, although the interface tends to smoothen with increasing isocyanate index. This picture holds, despite the absence of classical maxima in the SAXS patterns, easily misinterpreted as a sign of phase mixing.

According to our view, fractal symmetry arises from competition between incipient crosslinking and strong phase segregation tendencies. The competition eventually results in a significant degree of energetic 'sharing' (mutual strain) accross the phase boundary. The resulting frozen-in morphology represents an early stage of the development towards a more regular spinodal phase segregation, as occuring in PU foam systems of lower crosslink density (e.g., flexibles). In our opinion, real-time SAXS measurements using synchrotron radiation[12] are well advised as the most elegant way to validate and expand the above qualitative picture of polymer morphology development in rigid PU foams.

APPENDIX

The Power Law Convolute in SAXS

Fractal scattering theory departs from an ideal binary (black and white) contrast: a point either does or does not belong to the fractal. Thus, the electron density profile always resembles a combination of block functions in cross-section. In the case of a surface fractal, it is the discontinuity of the block function that delineates its phase boundary.

As long as binary contrast is maintained, the decay exponent of the scattering curve cannot become more negative than −4. This realization is quite old: it is, in fact, a simple reformulation of Porod's law. Deviations from binary contrast were first considered by Ruland:[20] he introduced the concept of graduality. It introduces an extra convolution factor that produces a steeper decay of the scattering curve (negative deviation). For a Gaussian convolute it has the form:

$$C_{(\text{Ruland})} = \exp -(\sigma^2 q^2)$$

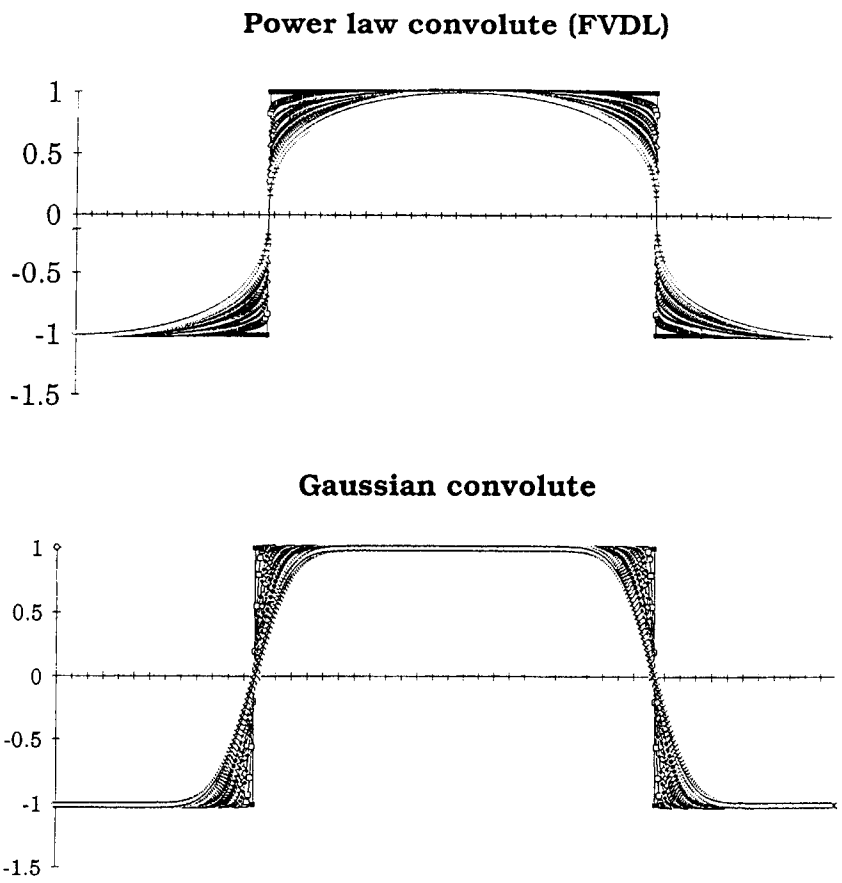

Figure A1 Binary electron density profile subjected to the two types of convolution. Notice the different behavior of the slope at the jump point.

In systems where the two phases only contain atoms of comparable scattering power, the electron density contrast relies heavily of the local density, i.e., the stacking of the monomers. For SAXS, this is the situation for most polymers. This point is more often neglected than quoted as a rationale, but the argument could certainly be made that the concept of graduality is one that merits consideration in polymers, solely because the stacking density is not necessarily a fixed quantity. Seen from this point of view, the steep decay we are confronted with is not really a surprise, and graduality is an obvious explanation to turn to.

Unfortunately, the specific profile Ruland introduced, the Gaussian convolute, is not a suitable vehicle to combine graduality with fractal scattering theory. It was introduced long before the latter made its entry and is not compatible. This is, e.g., seen from the fact that the Ruland convolution factor causes a downward curvature of a linear log–log plot. This is, however, only the outward manifestation in q-space of very fundamental problem: in real space, the Ruland profile lacks a discontinuity that marks the phase boundary that the (surface) fractal is trying to describe in terms of scaling properties. Diffuse mixing is often believed to cause this obliteration of the phase boundary.

Remedially, we propose a convolution factor of the simple power law form:

$$C_{\mathrm{FVDL}} = q^{-b}$$

Obviously, it was deliberately chosen such, that it leaves the linearity of the log–log plot intact. Despite its almost trivial shape in q-space, it actually represents a rather complicated operation on the density profile in real space. A typical resulting profile is shown in Figure A1. Mathematically, the real space operation involves fractional calculus;[22] more precisely, it is related to the two-sided broken integration proposed by Mandelbrot.[23,24] In terms of the differentiability of the profile this has consequences, essential to our problem.

A full account is given elsewhere,[19] but let us concentrate on the most important improvement. Both profiles are continuous, However, the Gaussian profile can be differentiated to any order without ever producing a discontinuity. For the power law profile, this is not so. In fact, a differentiation of broken order < 1 typically suffices to restore the block function's jump. Its position conveniently continues to define a discrete phase boundary (meniscus), the scaling properties of which the fractal model links to the state of segregation. This means that it is neither necessary nor desirable to invoke 'diffuse mixing,' a concept alien to this fractal description.

Instead, we propose that the profile represents a fully segregated situation, i.e. 'chemically' a binary contrast is maintained, so that the description of the state of phase segregation is entirely left to the fractal theory. The graduality results only from the fact that the two phases do not immediately reach their respective ideal bulk density values in a zone straddling the meniscus. This zone of deviating densities, one compressed, the other rarified relative to the bulk, we call the free volume double layer (FVDL). As density deviations relative to bulk can be interpreted as a strain, we can also speak of interfacial strain for the phenomenon as a whole.

The authors are grateful to Mr. Ad Kimenai and Mr. Bob Vastenhout for carrying out SAXS and TEM measurements, respectively. Stimulating discussions with Drs. Tony Ryan, Mike Elwell, and Adrian Birch are gratefully acknowledged.

REFERENCES

1. G. F. Smits and J. A. Thoen, *Proc. SPI/ISOPA World Congress*, 412 (1991).
2. W. A. Kaplan and R. L. Tabor, *Cell. Polym.*, **12,** 102 (1993).
3. H. Xiao, Z. H. Ping, J. W. Xie, T. Y. Yu, *J. Appl. Polym. Sci.*, **40,** 1131 (1990).
4. M. Pegoraro, L. Zanderighi, A. Penati , F. Severini, F. Bianchi, N. Cao , R. Sisto, and C. Valentini, *J. Appl. Polym. Sci.*, **43,** 687 (1991).
5. G. Galland and T. M. Lam, *J. Appl. Polym. Sci.*, **50,** 1041 (1993).
6. G. L. Wilkes, S. Abouzahr, and D. Radovich, *J. Cell. Plast.*, **19,** 248 (1983).
7. J. P. Armistead, G. L. Wilkes, and R. B. Turner, *J. Appl. Polym. Sci.*, **35,** 601 (1988).
8. D. Tyagi, G. L. Wilkes, B. Lee, and J. E. McGrath, in *Adv. Elastomers Rubber Elasticity (Proc. Symp.)*, Plenum, New York, 1985, p. 103.
9. A. Takahara, T. Kajiyama, and M. Sato, *Pol. Commun.*, **29,** 194 (1988).
10. H. J. M. Grünbauer, J. A. Thoen, J. C. W. Folmer, and H. C. van Lieshout, *J. Cell. Plast.*, **28,** 36 (1992).
11. D. W. Schaefer, B. C. Bunker, J. P. Wilcoxon, *Proc. R. Soc. Lond. A*, **423,** 35 (1989).
12. M. J. Elwell, A. J. Ryan, H. J. M. Grünbauer, H. C. van Lieshout, and J. A. Thoen, *Cellular Polymers*, International Symposium, Edinburgh, 1993.
13. J. W. C. van Bogart, A. Lilaonitkul, and S. L. Cooper, in *Multiphase Polymers*, Vol. 176, Adv. Chem. Ser., 1979.
14. T. P. Russell, D. S. Lees, T. Nishi, and S. C. Kim, *Macromolecules*, **26,** 1922 (1993).
15. R. Bonart and E. H. Müller, *J. Macromol. Sci.- Phys.*, **B10**(1), 177 (1974).
16. Y. Li, T. Gao, J. Liu, K. Linliu, C. R. Desper, and B. Chu, *Macromolecues*, **25,** 7365–7372 (1992).
17. P. W. Schmidt, in *The Fractal Approach to Heterogeneous Chemistry*, D. Avnir, Ed., John Wiley, New York, 1989.
18. S. M. Aharoni, N. S. Murthy, K. Zero, and S. F. Edwards, *Macromolecules*, **23,** 2533 (1990).
19. J. C. W. Folmer and D. Porter, to appear.
20. W. Ruland, *J. Appl. Crystl.*, **4,** 70–73 (1971).
21. C. G. Vonk, in *Small Angle X-Ray Scattering*, O. Glatter and O. Kratky, Eds., Academic Press, London, 1982.
22. K. B. Oldham and J. Spanier, in *Mathematics in Science and Engineering*, Vol. 111, R. Bellman, Ed., Academic Press, New York, 1974.
23. B. Mandelbrot, *The Fractal Geometry of Nature*, Freeman, San Francisco, 1982.
24. B. Mandelbrot, in *Encyclopedia of Statistical Sciences*, Vol. 3, S. Kotz and N. L. Johnson, Eds., J. Wiley & Sons, New York, 1983, p. 196ff.

Received November 20, 1993
Accepted May 10, 1994